Supplement of Hydrol. Earth Syst. Sci., 24, 2379–2398, 2020
https://doi.org/10.5194/hess-24-2379-2020-supplement

Hydrology and Earth System Sciences
Open Access
EGU

Supplement of

Modeling inorganic carbon dynamics in the Seine River continuum in France

Audrey Marescaux et al.

Correspondence to: Audrey Marescaux (audreymarescaux@gmail.com)

S1: List of state variables for the RIVE model

GROUP *	VARIABLE	DESCRIPTION
	Q	mean discharge during the 10 day period in $m^3 s^{-1}$
PHY	DIA	diatom biomass in mgC l^{-1}
	GRA	green algae (chlorophyceae) biomass in mgC l^{-1}
	CYA	cyanobacteria biomass in mgC l^{-1}
	MES	mineral suspended solid in mg l^{-1}
NUTS	NO3	nitrates in µmol l^{-1}
	NH4	ammonium in µmol l^{-1}
	PO4	phosphates in µmol l^{-1}
	PIT	total inorganic phosphorus in µmolP l^{-1} [**]
	SIO	dissolved silica in µmol l^{-1}
	OXY	dissolved oxygen in µmol l^{-1}
ZOO	ZOR	rotiferan-like zooplankton in mgC l^{-1}
	ZOC	cladoceran-like zooplankton in mgC l^{-1}
BACT	BAG	heterotrophic bacteria > 1µ in mgC l^{-1}
	BAP	heterotrophic bacteria <1µ in mgC l^{-1}
	NIT	ammonium oxidizing nitrifying bacteria in mgC l^{-1}
	NAT	nitrite oxidizing nitrifying bacteria in mgC l^{-1}
OC	DOC1	rapidly biodegradable dissolved organic matter in mgC l^{-1}
	DOC2	slowly biodegradable dissolved organic matter in mgC l^{-1}
	DOC3	refractory dissolved organic matter in mgC l^{-1}
	POC1	rapidly biodegradable particulate organic matter in mgC l^{-1}
	POC 2	slowly biodegradable particulate organic matter in mgC l^{-1}
	POC 3	refractory particulate organic matter in mgC l^{-1}
	DSS	low molecular weight directly assimilable organic substrates in mgC l^{-1}
Benthic	SIB	biogenic non-living particulate (amorphous) silica in µmol l^{-1}
	BOC1	benthic (deposited) rapidly biodegradable organic matter in gC m^{-2}
	BOC2	benthic (deposited) slowly biodegradable organic matter in gC m^{-2}
	BOC3	benthic (deposited) refractory organic matter in gC m^{-2}
	BPI	benthic (deposited) inorganic phosphorus in mmolP m^{-2}
	BBS	benthic (deposited) biogenic silica in mmol m^{-2}
	BFE	benthic (deposited) faecal bacteria in 1000 m^{-2} l^{-1}
	SED	deposited inorganic material in g m^{-2}
	FEL	free living faecal bacteria in nb l^{-1}
	FEA	attached faecal bacteria in nb l^{-1}
	N2O	nitrous oxide in µmol l^{-1}
	NO2	nitrite in µmol l^{-1}
	CH4	methane in µmol l^{-1}
IC	CO2 (***)	Carbon dioxide in mgC l^{-1}
	TA (***)	Total alkalinity in µmol l^{-1}
	DIC (***)	Dissolved inorganic carbon in mgC l^{-1}

(*) "Group" refer to generic group name provided in Figure 2 in this paper
(**) An instantaneous equilibrium is considered for adsorption of ortho-phosphate on MES, so that PIT is the only primary state variable to be considered.
(***) New state variable added in the RIVE model
All biomasses (DIA, GRA, CYA, BAG, BAP, NIT, NAT, ZOR, ZOC) as well as organic matter pools (DOC 1-2-3, POC 1-2-3, BOC 1-2-3) are considered to have constant massic C:N ratios, namely C/N=7

S2: Modeling objects of the Seine basin

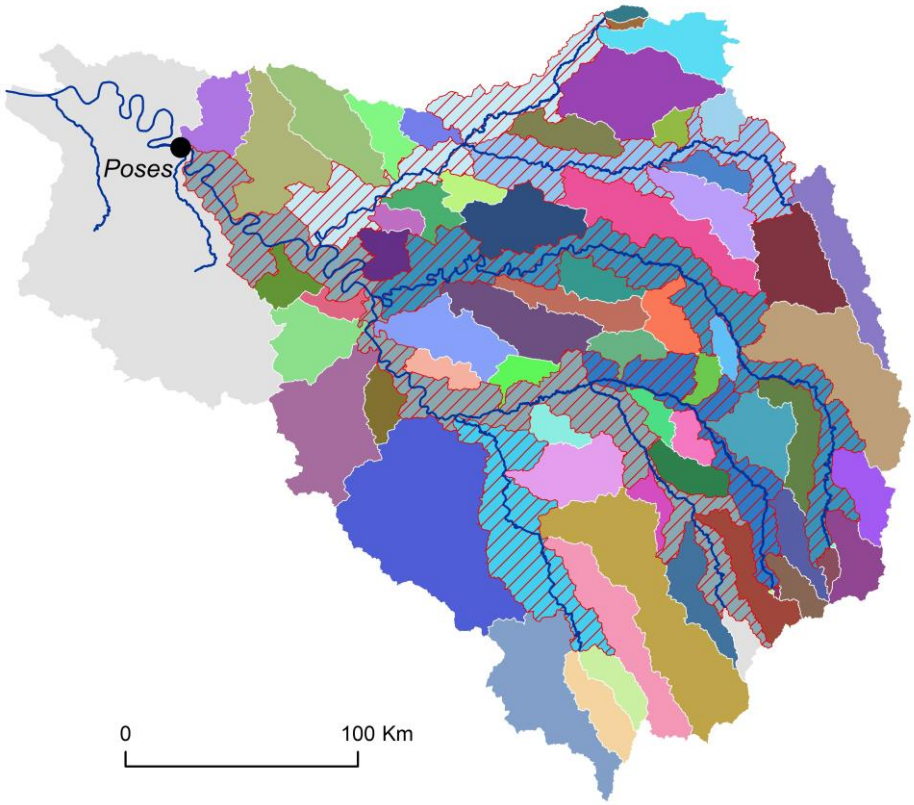

Figure S2- 1. PyNuts-Riverstrahler modeling objects. 6“Axis” objects (main river branches, mapped with red hatching) and 63 “basin” objects (upstream tributaries connected to “axis” objects).

Table S2- 2. List and morphological characteristics of the PyNuts-Riverstrahler modeling objects.

Id	Object type	Strahler order	Area km2	Number of riv. streches	Cum length km	Surf. Mirror km2
1	AXIS	4 - 7	5525	4	566	65.4
2	AXIS	2 - 5	1794	4	217	7.0
3	AXIS	5 - 6	2356	2	169	10.5
4	AXIS	3 - 6	4508	4	481	28.7
5	AXIS	3 - 6	2685	4	248	15.7
6	AXIS	5 - 5	2471	1	244	13.0
7	BASIN	1 - 4	225	24	105	0.4
8	BASIN	1 - 3	668	23	150	0.8
9	BASIN	1 - 4	738	53	287	1.8
10	BASIN	1 - 3	235	18	117	0.3
11	BASIN	1 - 3	462	38	191	0.7
12	BASIN	1 - 2	294	6	53	0.3
13	BASIN	1 - 3	287	18	121	0.4
14	BASIN	1 - 5	4182	270	1659	8.4
15	BASIN	1 - 3	311	27	154	0.5
16	BASIN	1 - 2	390	5	46	0.3
17	BASIN	1 - 4	1934	47	340	3.0
18	BASIN	1 - 4	937	80	417	1.6
19	BASIN	1 - 4	1035	80	538	2.7
20	BASIN	1 - 2	220	7	58	0.2
21	BASIN	1 - 3	387	13	75	0.3
22	BASIN	1 - 4	388	39	181	0.6
23	BASIN	1 - 4	1472	68	419	2.4
24	BASIN	1 - 3	755	18	141	0.6
25	BASIN	1 - 1	14	1	4	0.0
26	BASIN	1 - 1	4	1	2	0.0
27	BASIN	1 - 3	332	28	159	0.5
28	BASIN	1 - 4	481	29	169	0.7
29	BASIN	1 - 5	842	82	456	1.7
30	BASIN	1 - 3	289	25	126	0.4
31	BASIN	1 - 2	217	4	38	0.2
32	BASIN	1 - 2	241	3	45	0.3
33	BASIN	1 - 3	380	15	115	0.5
34	BASIN	1 - 4	443	76	312	0.9
35	BASIN	1 - 4	616	129	443	1.3
36	BASIN	1 - 5	1985	177	898	4.6
37	BASIN	1 - 4	1367	96	556	4.2
38	BASIN	1 - 5	3076	219	1257	8.6
39	BASIN	1 - 3	990	22	171	1.1
40	BASIN	1 - 3	113	11	41	0.1
41	BASIN	1 - 1	4	1	1	0.0
42	BASIN	1 - 4	625	56	255	1.2
43	BASIN	1 - 4	630	29	193	1.0
44	BASIN	1 - 3	688	29	222	1.1
45	BASIN	1 - 5	2183	135	887	4.3
46	BASIN	1 - 2	220	7	55	0.2
47	BASIN	1 - 3	486	9	110	0.6
48	BASIN	1 - 4	466	42	203	0.7
49	BASIN	1 - 3	632	47	245	1.1
50	BASIN	1 - 4	1083	82	452	1.9
51	BASIN	1 - 4	1196	96	534	2.7
52	BASIN	1 - 2	62	7	47	0.1
53	BASIN	1 - 3	99	14	90	0.2
54	BASIN	1 - 4	919	92	564	2.6
55	BASIN	1 - 4	1743	84	563	3.0
56	BASIN	1 - 4	578	75	325	1.0
57	BASIN	1 - 2	285	7	42	0.2
58	BASIN	1 - 3	299	19	85	0.3
59	BASIN	1 - 3	482	12	93	0.4
60	BASIN	1 - 4	1218	68	358	2.0
61	BASIN	1 - 3	415	16	93	0.4
62	BASIN	1 - 3	211	11	70	0.2
63	BASIN	1 - 4	1050	86	511	2.3
64	BASIN	1 - 4	1230	127	663	2.8
65	BASIN	1 - 4	330	36	202	0.5
66	BASIN	1 - 2	209	4	34	0.2
67	BASIN	1 - 2	335	6	59	0.4
68	BASIN	1 - 3	837	14	141	1.0
69	BASIN	1 - 4	1480	86	487	2.9

S3: Description of the inorganic carbon module implemented in pyNuts-Riverstrahler

3.1. The carbonate systems

The major dissolved forms of the carbonate system are CO_2 (aq) aqueous carbon dioxide, H_2CO_3 (aq) carbonic acid, HCO_3^- (aq) bicarbonate ion, CO_3^{2-} (aq) carbonate ion.

$$CO_2(g) \rightleftharpoons CO_2(aq) \quad \text{Eq. S1}$$

$$CO_2(aq) + H_2O\ (aq) \rightleftharpoons H_2CO_3\ (aq) \rightleftharpoons HCO_3^-(aq) + H^+(aq) \quad \text{Eq. S2}$$

$$HCO_3^-(aq) \rightleftharpoons CO_3^{2-}(aq) + H^+(aq) \quad \text{Eq. S3}$$

The acid dissolution constants from the second and the third equations are, respectively:

$$K_1 = \frac{[H^+][HCO_3^-]}{[CO_2]} \quad \text{Eq. S4}$$

$$K_2 = \frac{[H^+][CO_3^{2-}]}{[HCO_3^-]} \quad \text{Eq. S5}$$

3.2. Carbonate system as a function of DIC

Carbonate dissociation can be determined by total inorganic carbon.

$$DIC = [CO_2] + [HCO_3^-] + [CO_3^{2-}] \quad \text{Eq. S6}$$

With the insertion of [4] and [5] in [7], DIC becomes:

$$DIC = \frac{[H^+][HCO_3^-]}{K_1} + [HCO^{3-}] + \frac{[HCO_3^-]K_2}{[H^+]} \quad \text{Eq. S7}$$

$$\leftrightarrow [HCO_3^-] = \frac{DIC}{\frac{[H^+]}{K_1} + \frac{K_2}{[H^+]} + 1} \quad \text{Eq. S8}$$

and with $[HCO_3^-]$, we can calculate $[CO_3^{2-}]$ and $[CO_2]$ with [8] and [9].

$$[CO_2] = \frac{[H^+]}{K_1} \frac{DIC}{\frac{[H^+]}{K_1} + \frac{K_2}{[H^+]} + 1} \quad \text{Eq. S9}$$

$$[CO_3^{2-}] = \frac{K_2}{[H^+]} \frac{DIC}{\frac{[H^+]}{K_1} + \frac{K_2}{[H^+]} + 1} \quad \text{Eq. S10}$$

3.3. The dissociation constants of carbonic acid

According to Millero et al. (2006), Harned and Scholes (1941), Harned et al. (1943) the dissociation constants of carbonic acid (molar concentration unit) are calculated as:

$$pK_1 = -126.34048 + \frac{6320.813}{T_K} + 19.568224 * ln(T_K) \quad \text{Eq. S11}$$

$$pK_2 = -90.18333 + \frac{5143.692}{T_K} + 14.613358 * \ln(T_K) \quad \text{Eq. S12}$$

where T_k is the water temperature in Kelvin (°K).

and:

$$K_1 = 10^{-pK_1} \quad \text{Eq. S13}$$

$$K_2 = 10^{-pK_2} \quad \text{Eq. S14}$$

3.4. pH calculation

In the pyNuts-Riverstrahler model, pH had not yet been calculated. In the inorganic carbon module, we added the calculation of pH derived from Culberson (1980) to calculate the speciation of carbonate (Eqs. 9–11). The equations of Culberson were derived with the assumption that only bicarbonates, carbonates and borates contribute to TA. The author specifies that phosphate concentration < 3.10^{-6} mol L^{-1} and silicate at concentrations < 50.10^{-1} mol L^{-1} have negligible effect on the calculation of the pH (< ~0.001 pH). In addition, total dissolved boron concentration can generally be ignored in freshwaters (Emiroglu et al., 2010).

$$DIC_{conv} = \frac{DIC}{12\ rho}\ 10^6 \quad \text{Eq. S15}$$

DIC_{conv} (conversion from mgC L^{-1} to µmol kg^{-1}), where rho (kg m^{-3}) is the water density from Millero and Poisson, 1981)

$$Xdiss = \left(1 - \frac{Bor0}{TA}\right).K_b + \left(1 - \frac{DIC_{conv}}{TA}\right).K_1 \quad \text{Eq. S16}$$

$$Ydiss = \left(1 - \frac{Bor0 + DIC_{conv}}{TA}\right).K_1.K_b + \left(1 - 2.\frac{DIC_{conv}}{TA}\right).K_1.K_2 \quad \text{Eq. S17}$$

$$Zdiss = \left(1 - \frac{Bor0 + 2.DIC_{conv}}{TA}\right).K_1.K_2.K_b \quad \text{Eq. S18}$$

$$aCulb = \frac{(Xdiss^2 - 3.Ydiss)}{9} \quad \text{Eq. S19}$$

$$bCulb = \frac{-(2Xdiss^3 - 9.Xdiss.Ydiss + 27.Zdiss)}{54} \quad \text{Eq. S20}$$

$$phyCulb = cos(\frac{bCulb}{(aCulb^3)^{0.5}}) \quad \text{Eq. S21}$$

$$[H_3O^+] = 2.aCulb^{0.5}.cos\left(\frac{phyCulb}{3}\right) - \frac{Xdiss}{3} \quad \text{Eq. S22}$$

$$pH = -\log_{10}[H_3O^+] \quad \text{Eq. S23}$$

where Bor0 is the total dissolved boron concentration that can generally be ignored in freshwaters (Emiroglu et al., 2010). “Xdiss”, “Ydiss”, “Zdiss” are the coefficient of the general cubic equation. “aCulb” and “bCulb” are the zero of the general cubic equation. H_3O^+ is the positive roots of the general cubic equation that can be calculated from phyCulb (where arc cos(phyCulb) is the inverse trigonometric function) (see Culberson et al. 1980).

3.5. CO_2 flux calculation

The carbonate speciation function makes it possible to calculate the concentration in aqueous carbon dioxide (CO_2) (Eq. S9).

The flux (gC m^{-2} h^{-1}) of CO_2 at the interface of the river and the atmosphere is calculated as:

$$F_{CO_2} = \frac{k}{24} \, (CO_2 - CO_2atm).rho.10^{-3} \qquad \text{Eq. S24}$$

Monthly atmospheric CO_2 (CO_2atm, mgC L^{-1}) was measured at Mauna Loa Observatory (Hawaii, USA) and provided by the NOAA/ESRL: (http://www.esrl.noaa.gov/gmd/ccgg/trends/, last accessed 2020/02/11), Scripps Institution of Oceanography (scrippsco2.ucsd.edu/, last accessed 2018/11/05). Concentrations in ppm from Mauna Loa Observatory were converted to mgC L^{-1} using solubility according to Weiss, (1974). The CO_2 concentration in water (CO_2) (mgC L^{-1}) was calculated according to section 3.2. Carbonate system as a function of DIC". rho ($kg\ m^{-3}$) is the water density calculated by the International One Atmosphere Equation (Millero and Poisson, 1981).

The flux of CO_2 depends on the gas transfer velocity (k) that can be determined from the temperature-normalized gas transfer velocity (k_{600}). k_{600} is the gas transfer velocity at a water temperature of 20°C. Parametrization related to the gas exchange used k_{600} to compare systems excluding temperature's physical effect. According to Wilke and Chang (1955) and Wanninkhof (1992), the gas transfer velocity k(m d^{-1}) can be calculated as:

$$k = k_{600} \cdot \sqrt{\frac{600}{Sc_{CO_2}(T)}} \qquad \text{Eq. S25}$$

k_{600} is the gas transfer velocity for a Schmidt number of 600 (m d^{-1}), and $Sc_{CO_2}(T)$ is the Schmidt number (dimensionless) calculated with the water temperature (T) in Celsius ($°C$) calculated as:

$$Sc_{CO_2}(T) = 1911.1 - 118.11T + 3.4527T^2 - 0.04132T^3 \quad \text{Eq. S26}$$

For rivers less than 100 m wide (SO 1–5), the k_{600} equation used was retrieved from Alin et al. (2011):

$$k_{600} = \frac{13.82 + 0.35v * 100}{100} \quad \text{Eq. S27}$$

where k_{600} (m h^{-1}) depends on v, the water velocity (m s^{-1}).

In general, k_{600} equations for rivers of widths greater than 100 m require wind velocity (e.g., Chu and Jirka, 2003; Alin et al., 2011; Raymond et al., 2012a). At this stage the pyNuts Riverstrahler model does not consider the wind as an input, which would have required a much higher spatiotemporal resolution to reflect its heterogeneity in the Seine basin with the diurnal cycle affected by phenomena such as breeze (Quintana-Seguí et al., 2008). Therefore, for river widths greater than 100 m, the k_{600} equation from O'Connor and Dobbins, (1958) and Ho et al. (2016), neglecting the term related to the wind, was selected (see Eq. S28):

$$k_{600} = \frac{a\sqrt{\frac{v}{depth}}}{100} \quad \text{Eq. S28}$$

where k_{600} (m h^{-1}) depends on v, the water velocity (m s^{-1}), and the river depth (m) and the coefficient "a". The coefficient was tested from 0 to 2 for SO6 and SO7. We found that SO6 showed a behavior near the original coefficient of 1.539 from O'Connor and Dobbins (1958) with 1.55, and SO7 a behavior near the 0.77 proposed by and Ho et al. (2016) with 0.55.

3.6. Parameters, constants and equations used in the inorganic carbon module.

Table S3-1 Parameters used in the inorganic carbon module for freshwaters

Parameters	Acronym	Units	Sources
Dissociation constants of carbonic acid	K_1, K_2	µmol l^{-1}	Harned and Scholes (1941), Harned et al. (1943), and, Millero et al. (2006)
Solubility	k0	mol kg^{-1} atm^{-1}	Weiss (1974)
gas transfer velocity	*k-value*	m h^{-1}	Wanninkhof (1992), Wilke and Chang (1955) Alin et al. (2011, Eq. S27 for river width inferior to 100m) and O'Connor and Dobbins (1958) updated in Ho et al. (2016), for river width superior to 100m.
water density	Rho	kg m^{-3}	Millero and Poisson (1981)
pH	pH	-	Culberson (1980)
Apparent ionization constant of boric acid	Kb	hPa	Schubert (2011)

S4 Representation of superficial MESO water bodies

Groundwaters are under strong anthropogenic pressures due to water withdrawn for drinking water production and pollution by agriculture. The European directive (Water Framework Directive 2000/60/CE) aims to reach the good environmental status of surface and groundwaters and has introduced the notion of groundwater bodies (French acronym: Masse d'Eau SOuterraine - MESO) (Figure S4-1). These MESO units are defined by hydrogeological criteria (e.g., extent and characteristics of the geological layers, feeding area, hydraulic connection between geological layers, interaction with surface waters and associated terrestrial ecosystems, etc.) and nonhydrogeological criteria (capture or the possibility of capture; impact of pressures, potential pollution, administrative boundaries, etc.). The status and upward trends in the concentrations of any pollutant in groundwaters are monitored at the MESO scale. The Seine basin includes 48 unconfined (fully or partially) MESO units (see map), which were regrouped according to the lithology and geological ages (colors) to simplify the representation.

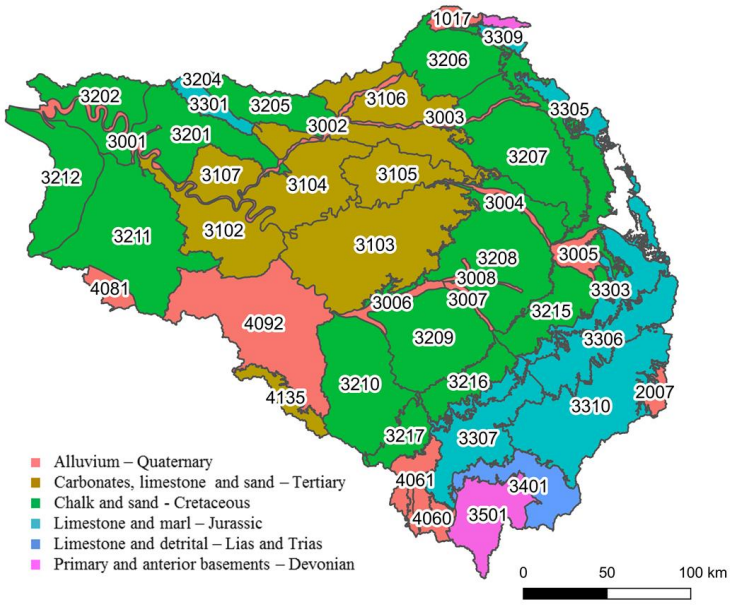

Figure S4-1. Superficial MESO (Masse d'Eau SOuterraine) water bodies of the Seine basin grouped according to the lithology and geological ages

Table S4-1 Mean concentrations and standard deviations of total alkalinity (TA, µmole L^{-1}) and dissolved inorganic carbon (DIC, mgC L^{-1}) grouped by MESO units in the Seine Basin for the 2010-2013 period.

MESO code	**Dominant lithology and geological age**	**TA (µmole L^{-1})**		**DIC (mgC L^{-1})**	
		mean	*sd*	*mean*	*sd*
1017	Alluvium - Quaternary	5113	388	79	3
2007		4454	671	75	7
3001		4030	1018	71	12
3002		5058	677	85	6
3003		5288	1025	90	11
3004		4532	992	72	10
3005		4624	487	79	8
3006		3960	493	69	7
3007		4254	382	67	7
3008		4274	832	70	10
4060		4701	291	74	2
4061		4701	291	74	2
4081		1568	1462	35	16
4092		4245	785	72	10
3102	carbonate, limestone and sand – Tertiary	4719	878	81	15
3103		5453	988	76	11
3104		5580	673	92	10
3105		5387	768	91	7
3106		5321	360	89	10
3107		5264	488	86	5
4135		3774	1011	64	11
3201	chalk and sand - Cretaceous	5264	488	83	4
3202		4574	546	76	6
3204		4831	389	81	1
3205		5192	470	83	5
3206		5134	576	83	7
3207		4268	941	70	11
3208		3911	866	64	10
3209		4169	680	69	8
3210		4669	590	75	6
3211		4173	801	67	10
3212		4713	401	77	4
3214		5172	941	87	12
3215		4394	1202	73	13
3216		4732	1011	77	11
3217		5002	481	77	4
3218		4590	995	75	12
3301	Limestone and marl - Jurassic	1660	346	41	5
3303		5120	467	82	6
3304		4939	265	78	4
3305		5236	971	88	12
3306		4629	754	77	8
3307		4907	585	80	6
3309		4938	365	81	4
3310		4454	671	75	7
3401	Limestone and detrital – Lias and Trias	5053	699	82	8
3501	Primary and anterior basements - Devonian	765	228	25	4
3508		663	683	27	9

S5: Sampling strategy and protocol for measuring emissions from wastewater treatment plants in the Seine basin

Table S5-1. Location of the sampled WWTPs. Their nominal capacity and type of treatment are retrieved from http://assainissement.developpement-durable.gouv.fr/, last accessed 2019/03/07. Measured values for TA, DIC, pH and pCO_2.

WWTPs	Location	Nominal capacity (Inhab. Eq.)	Water treatment	TA (µmole L^{-1})	DIC (mgC L^{-1})	pH	pCO_2 (ppmv)
Butry	49°04'60N, 2°12'00E	6700	Low load actived sludge	5885	76.27	7.3	31723
Auvers	49°04'00N, 2°10'00E	34,300	Secondary treatment, denitrification, dephosphatation	3700	53.39	7.26	28723
Dammarie	48°30'57"N, 2°36'43"E	80,000	Secondary treatment, denitrification, dephosphatation	4800	68.55	7.45	17268
Rosny	49°0'7"N, 1°39'11"E	135,417	Secondary treatment, denitrification, dephosphatation	4500	55.50	7.4	18651
Troyes	48°20'5"N, 4°2'37"E	260,000	Secondary treatment, denitrification, dephosphatation	#N/A	86.31	7.4	29930
Seine Centre	48°55'58"N, 2°14'43"E	800,000	Secondary treatment, denitrification, dephosphatation	3590	47.44	8.17	#N/A
St-Thibault-des-Vignes	48°52'20"N, 2°40'27"E	350,000	Secondary treatment, denitrification, dephosphatation	5660	73.55	7.40	15732
SAV	48°58′25″ N, 2°09'56"E	7,500,000	Secondary treatment, denitrification, dephosphatation	2915	#N/A	7.91	#N/A
Inputs of the model (weighted average per capacity):				3993	69.75		

Water samples were filtrated on combusted filters (4 h at 500°C: GF/F 0.7 µm, 25 mm), and filtrates enabled measurement of DIC and TA concentrations. Dissolved inorganic carbon was analyzed with a TOC analyzer (Aurora 1030). Nongaseous DIC analyses required acidification of the filtrated sample by adding sodium persulfate reagents (100 g L^{-1}) to dissociate the carbonate in the CO_2 that was detected with nondispersive infrared gas analysis (IRGA). TA (µmol kg-1) was analyzed using an automatic titrator (TitroLine® 5000) on three 20-mL replicates of filtered water (GF/F: 0.7 µm), with hydrochloric acid (0.1 M).

References of the Supplementary Information

Alin, S.R., Rasera, M.M.D.F.F.L., Salimon, C.I., Richey, J.E., Holtgrieve, G.W., Krusche, A. V., Snidvongs, A., 2011b. Physical controls on carbon dioxide transfer velocity and flux in low-gradient river systems and implications for regional carbon budgets. J. Geophys. Res. 116, 17. doi:G01009 10.1029/2010jg001398

Chu, C.R., Jirka, G.H., 2003. Wind and Stream Flow Induced Reaeration. J. Environ. Eng. 129, 1129–1136. doi:10.1061/(ASCE)0733-9372(2003)129:12(1129)

Culberson, C.H., 1980. Calculation of the in situ pH of seawater. Limnol. Oceanogr. 25, 150–152. doi:10.4319/lo.1980.25.1.0150

Emiroglu, O., Cicek, A., Arslan, N., Aksan, S., Rüzgar, M., 2010. Boron concentration in water, sediment and different organisms around large borate deposits of Turkey. Bull. Environ. Contam. Toxicol. 84, 427–431. doi:10.1007/s00128-010-9961-8

Harned, H.S., Davis, R.J., Jr., R.D., 1943. The ionization constant of carbonic acid in water and the solubility of carbon dioxide in water and aqueous salt solutions from 0 to 50°. J. Am. Chem. Soc. 65, 2030–2037.

Harned, H.S., Scholes, S.R., 1941. The Ionization Constant of HCO3- from 0 to 50°. J. Am. Chem. Soc. 63, 1706–1709. doi:10.1021/ja01851a058

Ho, D.T., Coffineau, N., Hickman, B., Chow, N., Koffman, T., Schlosser, P., 2016. Influence of current velocity and wind speed on air-water gas exchange in a mangrove estuary. Geophys. Res. Lett. 43, 3813–3821. doi:10.1002/2016GL068727.Received

Millero, F.J., Graham, T.B., Huang, F., Bustos-Serrano, H., Pierrot, D., 2006. Dissociation constants of carbonic acid in seawater as a function of salinity and temperature. Mar. Chem. 100, 80–94. doi:10.1016/j.marchem.2005.12.001

Millero, F.J., Poisson, A., 1981. International one-atmosphere equation of state of seawater. Deep Sea Res. Part A, Oceanogr. Res. Pap. 28, 625–629. doi:10.1016/0198-0149(81)90122-9

O'Connor, D.J., Dobbins, W.E., 1958. Mechanism of reaeration in natural streams. Trans. Am. Soc. Civ. Eng. 123, 641–684.

Quintana-Seguí, P., Le Moigne, P., Durand, Y., Martin, E., Habets, F., Baillon, M., Canellas, C., Franchisteguy, L., Morel, S., 2008. Analysis of near-surface atmospheric variables: Validation of the SAFRAN analysis over France. J. Appl. Meteorol. Climatol. 47, 92–107. doi:10.1175/2007JAMC1636.1

Raymond, P.A., Zappa, C.J., Butman, D., Bott, T.L., Potter, J., Mulholland, P., Laursen, A.E., McDowell, W.H., Newbold, D., 2012. Scaling the gas transfer velocity and hydraulic geometry in streams and small rivers. Limnol. Oceanogr. Fluids Environ. 2, 41–53. doi:10.1215/21573689-1597669

Schubert, D., 2011. Boron Oxides, Boric Acid, and Borates, Kirk-Othmer Encyclopedia of Chemical Technology. doi:10.1002/0471238961.0215181519130920.a01.pub3

Wanninkhof, R., 1992. Relationship Between Wind Speed and Gas Exchange. J. Geophys. Res. 97, 7373–7382. doi:10.1029/92JC00188

Weiss, R.F., 1974. Carbon dioxide in water and seawater: the solubility of a non-ideal gas. Mar. Chem. 2, 203–215. doi:10.1016/0304-4203(74)90015-2

Wilke, C.R., Chang, P., 1955. Correlation of diffusion coefficients in dilute solutions. AIChE J. 1, 264–270. doi:10.1002/aic.690010222